Identification of a methanol-inducible promoter from *Rhodococcus erythropolis* PR4 and its use as an expression vector

Yusuke Kagawa[1, 2], Yasuo Mitani[3], Hea-Yeon Yun[1, 2], Nobutaka Nakashima[1], Noriko Tamura[1], and Tomohiro Tamura[1, 2*]

[1]*Bioproduction Research Institute, National Institute of Advanced Industrial Science and Technology (AIST), Tsukisamu-Higashi, Toyohira-ku, Sapporo 062-8517, Japan*

[2]*Graduate School of Agriculture, Hokkaido University, Kita-9, Nishi-9, Kita-ku, Sapporo 060-8589, Japan*

[3]*Bioproduction Research Institute, National Institute of Advanced Industrial Science and Technology (AIST), Tsukuba Central 6-10, Tsukuba, Ibaraki 305-8566, Japan*

*Corresponding author. Phone: +81-11-857-8938. Fax: +81-11-857-8980. E-mail: t-tamura@aist.go.jp

Ruuning title : Methanol-inducible promoter from Rhodococcus

Key words : promoter; expression; methanol-inducible; RamB; *Rhodococcus erythropolis*

Abstract

The genus *Rhodococcus* exhibits a broad range of catalytic activity and is tolerant to various kinds of organic solvents. This property makes rhodococci suitable for use as a whole-cell catalyst. Various tools for genetic engineering have been developed to use *Rhodococcus erythropolis* as a host for bioconversion. In this study, we investigated the protein expression responses of *R. erythropolis* strains and found that isocitrate lyase production in *R. erythropolis* PR4 (ICL_{Re}) was induced by methanol. By analyzing the regulation mechanisms of icl_{Re} expression, the ~200-bp upstream region from the first nucleotide of the translation initiation codon of icl_{Re} was shown to be sufficient for the methanol-inducible expression. Also, the ~100-bp upstream region exhibited strong constitutive promoter activity by an unknown mechanism(s). By investigating proteins that bound to the upstream region of icl_{Re} *in vitro*, a RamB homologue of *R. erythropolis* PR4 ($RamB_{Re}$) was identified. Moreover, 2 putative $RamB_{Re}$ binding sites were identified in the upstream region of icl_{Re} through pull-down assays. A $ramB_{Re}$ knockout experiment suggested that $RamB_{Re}$ negatively controlled the expression of icl_{Re} and that $RamB_{Re}$ regulation was dependent on the availability of a carbon source. On the basis of these findings, we were able to create novel methanol-inducible and strong constitutive expression vectors.

Introduction

The genus *Rhodococcus* belongs to mycolic-acid containing actinomycetes. Many members of the order *Actinomycetes* are known to be antibiotic producers, while rhodococci are known to exhibit a broad range of catalytic activity that has applications in industrial, pharmaceutical, and environmental biotechnology (1-4). For example, rhodococci have been used as biocatalysts for the industrial production of acrylamide (5). Rhodococci are often isolated from soils contaminated with crude oil and/or xenobiotic compounds, and these organisms can utilize such compounds as carbon sources. Moreover, they exhibit tolerance to various organic solvents (6-9).

Their solvent tolerance property makes rhodococci suitable for use as a whole-cell biocatalyst; this is particularly favorable for biocatalytic processes that require cofactor regeneration and/or involve multistep metabolic pathways (10). The 2-phase water-solvent system has been used for whole-cell bioconversion because it permits the efficient conversion of hydrophobic substrates, which are dissolved in the solvent phase, into final products. In most cases, the products are also hydrophobic and accumulate in the solvent phase; this enables continuous reaction and feasible purification (10-13). To date, both gram-positive and gram-negative organic solvent–tolerant bacteria have been used for such reactions (10, 11, 14). Although *Escherichia coli* is not particularly tolerant to solvents, it has been used for whole-cell bioconversion in the presence of toxic solvents because of its ease of handling (15). Nevertheless, rhodococci remain superior candidates for such applications owing to their diverse catabolic abilities and remarkable resistance to various solvents. Solvent-tolerant mechanisms have been investigated in various bacteria, particularly in gram-negative bacteria (16, 17).

Gram-negative bacteria have an outer cell membrane in addition to an inner cell membrane, and these 2 membranes create a periplasmic space between them. Such cell wall structure protects the cell from organic solvents that can damage the cell membrane by attacking the lipid bilayer (18).

To use *Rhodococcus erythropolis* as a host cell for bioproduction, various tools useful for genetic engineering have been developed, such as expression vectors containing an inducible promoter or a constitutive promoter, transposon mutagenesis and/or expression system, and gene expression analysis systems (19-25). To date, such tools have been successfully used in recombinant protein production and bioreactions in aqueous media (26, 27). To fully utilize the abilities of rhodococci, particularly their solvent tolerance property, a solvent-inducible promoter would be useful. If such a promoter is available, organic solvents can be used not only as reservoirs for the substrate and/or the product but also as inducers for proteins that are involved in the catalytic reactions. Therefore, we investigated the responses of various *R. erythropolis* strains to various kinds of organic solvents.

In this report, we identified isocitrate lyase from *R. erythropolis* PR4 (ICL_{Re}) as a methanol-inducible protein, and investigated its expression regulation mechanisms by analyzing the upstream region of icl_{Re}. Also, we identified a *RamB* homologue of *R. erythropolis* PR4 ($RamB_{Re}$) by isolating proteins that were bound to the upstream region of icl_{Re}. Finally, the upstream region of icl_{Re} was used to create methanol-inducible and strong constitutive expression vectors.

Materials and Methods

Bacterial strains and culture conditions

R. erythropolis strains PR4 and NI86/21 were obtained from the National Institute of Technology and Evaluation (NITE, Japan) and the National Collection of Agricultural and Industrial Microorganisms (Hungary), respectively. *R. erythropolis* strains JCM3201 and JCM6824 were obtained from the Japan Collection of Microorganisms. *E. coli* DH5α and XL1-blue were used as general cloning hosts. *R. erythropolis* and *E. coli* strains were routinely cultured in Luria-Bertani (LB) broth (1% Bacto tryptone, 0.5% Bacto yeast extract, and 1% NaCl) in the presence or absence of antibiotics at 28°C and 37°C, respectively. The antibiotics used to select transformants in the culture media were chloramphenicol (17 μg/mL), kanamycin (200 μg/mL), and ampicillin (50 μg/mL). If necessary, cell growth was monitored by measuring optical density at 600 nm (OD_{600}). In the plate culture, the medium was solidified by adding 1.5% agar.

Preparation of total protein

Single colony of *R. erythropolis* was inoculated into 10 mL LB mediun and incubated until it reached to a stationary phase. Then, the seed culture was inoculated into 100 mL fresh LB medium and incubated for 20 h at 28°C with shaking at 120 rpm in a 300 mL baffled flask. In order to increase the amount of cell culture, 100 mL

120 culture that was obtained by the previous step was inoculated into 1 L fresh LB medium
121 and incubated for 20 h at 28°C with shaking at 120 rpm in a 3 L baffled flask. A 20 mL
122 portion that was obtained from the culture in 3 L flask was transferred into a 50 mL
123 screw capped plastic tube (Corning inc., Corning, NY). Fifty microliters of *R.*
124 *erythropolis* seed culture was inoculated into 15 mL of LB medium and incubated for 2
125 days. Then, the organic solvent was added into the culture to a proportion of 1% or 5%,
126 and the culture was incubated for an additional 24 h. Cells were grown in a
127 screw-capped 50 mL plastic tube to prevent evaporation of organic solvents. The
128 organic solvents used in this study were ethanol, acetone, dimethyl sulfoxide, propanol,
129 butanol, methanol, acetonitrile, isopropyl acetate, 2-methyl-1-propanol, methyl ethyl
130 ketone, and ethyl acetate. The culture was harvested by centrifugation at 1500 × *g* for
131 10 min at 4°C. Then, cells were washed with 50 mM phosphate buffer (pH 7.5) and
132 resuspended in 500 μL of the same buffer. The cells were then disrupted using a Beads
133 shocker (Yasui-kikai, Osaka, Japan). The supernatant was collected by centrifugation at
134 20,817 × *g* for 10 min at 4°C and used as the total protein. Protein analysis was
135 performed through sodium dodecyl sulfate-polyacrylamide gel electrophoresis
136 (SDS-PAGE). Unless otherwise specified, 12.5% acrylamide was used for SDS-PAGE
137 and protein bands were visualized using Coomassie brilliant blue (CBB) staining.
138
139 *Two-dimensional gel electrophoresis (2-DE)*
140
141 Three milligrams of total protein was loaded onto a Superose-12 column (GE
142 Healthcare, Buckinghamshire, UK) equilibrated with 25 mM Tris-HCl (pH 7.5)

143 containing 10% glycerol. Then, a 50 μL fraction with a high amount of
144 methanol-inducible protein was resuspended in 75 μL of rehydration buffer containing
145 8 M urea, 2% 3-[(3-cholamidopropyl) dimethylammonio]-1-propanesulfonate, 0.5%
146 immobilized pH gradient (IPG) buffer, 0.002% bromophenol blue, 0.28% dithiothreitol,
147 and applied to pH 3–11 IPG strips (GE Healthcare) for overnight rehydration.
148 Isoelectronic focusing was performed using Ettan IPGphor II (GE Healthcare) under the
149 following conditions: 500 V for 1 h, 1000 V for 1 h, 8000 V for 3 h. IPG strips were
150 equilibrated with SDS equilibration buffer [6 M urea, 75 mM Tris-HCl (pH 8.8), 29.3%
151 glycerol, 2% SDS, 0.002% bromophenol blue]. The second-dimensional separation was
152 carried out by placing equilibrated IPG strips onto a SDS-PAGE gel that was sealed
153 with 0.5% (w/v) agarose.
154
155 *Liquid chromatography-mass spectrometry/mass spectrometry (LC-MS/MS)*
156
157 After 2-DE, the spot was excised and digested as described previously (28, 29).
158 Tryptic peptides were separated by reverse-phase chromatography using a MAGIC C18
159 column (3 μm, 200 Å, 0.2 mm i.d. × 150 mm; Michrom Bioresources, Auburn, CA)
160 connected to a MAGIC 2002 LC system (Michrom Bioresources). Peptides were loaded
161 onto a reverse-phase column as described previously (30) and then eluted during a
162 40-min linear gradient from 5% to 40% of solvent B (90% acetonitrile, 0.1% formic
163 acid) at a flow rate of 100 μL/min. The effluent was split by a MAGIC splitter
164 (Michrom Bioresources) to approximately 0.9 μL/min and introduced directly into an
165 LCQ-DECA XP plus ion trap mass spectrometer (Thermo Fisher Scientific, Waltham,

MA) equipped with a nanoelectrospray ion source (AMR, Tokyo, Japan). All tandem MS spectra were searched against the NCBI non-redundant database and analyzed using the TurboSequest algorithm in the BioWorks 3.2 software package (ThermoFisher Scientific, Waltham, MA) as described previously (30). The identified peptides were further evaluated using the following filters: peptide probability (≤1e-003), delta correlation score (≥0.1), and cross-correlation (X Corr) values (≥1.9, 2.2, 3.75 for 1+, 2+, 3+ charge-state peptides, respectively).

Cloning of the genes identified with LC-MS/MS

The degenerate primers DGP_S (5′-GAGGCKGCKACKCTKATCACKTCKGACGTKGACGA-3′) and DGP_AS (5′-CGGATGTGTTGTTGKGTKGGGATKAGKAC-3′) were designed corresponding to conserved regions of amino acid sequences of ICL. Degenerate PCR was performed for 25 cycles consisting of 94°C for 30 s, 68°C for 30 s, and 74°C for 2.5 min, with a final extension at 74°C for 7 min by using KOD Dash DNA polymerase (Toyobo, Osaka, Japan) and genome DNA as template. An ~150-bp product was purified and subcloned into a pBS-SK+ vector (Agilent Technologies, Santa Clara, CA) for sequencing. On the basis of the sequence obtained, primers were designed to amplify the full length of icl_{Re} by inverse PCR. For the inverse PCR, genomic DNA of *R. erythropolis* PR4 was digested with either *Bam*HI or *Nco*I, purified by a miniprep purification kit (Promega, Madison, WI), and circularized with Ligation kit solution I (Takara, Shiga, Japan). Inverse PCR was performed using KOD FX DNA polymerase

(Toyobo). The sequences of DNA fragments were analyzed by primer walking.

Reverse transcriptase-polymerase chain reaction (RT-PCR)

Total RNA was extracted from *R. erythropolis* PR4 grown in the presence of 5% methanol by using RNeasy Midi Kit (Qiagen, Hilden, Germany) and treated with RNase-free DNase I to remove genomic DNA followed by passing through an RNeasy minicolumn (Qiagen). RT-PCR reaction was performed using the Thermo Script RT-PCR System (Invitrogen, Carlsbad, CA) according to the manufacturer's manual. First strand synthesis was carried out using a random primer. PCR was performed using 5 pairs of primers corresponding to the fragments illustrated in Fig. 2B. For fragment a, icl_S (5′-AACCTCTCGGGCCACACGTA-3′) and crt_AS (5′-GCTCCTTGAACTCTTCGTACATGGAGT-3′); b, crt_S (5′-ACCAGCGAAAAAATTCAGCGCG-3′) and mhm_AS1 (5′-GCGCGCCTTCCTTGAGTGCTTCGAGAA-3′); c, mhm_S (5′-GGCAAGCGAATCGATCTCTCTCGATCG-3′) and adh_AS1 (5′-GCAGAAGTCGAGCATCTCCTGTGTCTG-3′); d, icl_S and mhm_AS2 (5′-AGGACTCGAGGGCGCGCTTGAGCTCA-3′); e, crt_S and adh_AS2 (5′-GTTCGATGCCCTCGGGGATCG-3′). RT-PCR products were analyzed on 1.0% agarose gel. For the negative control experiment, water was added instead of RT in the reaction and the product was used as a template for PCR. In the negative control experiment, no band was visible even after 40 cycles of PCR.

ICL activity assay

ICL activity was assayed spectrophotometrically at 324 nm using the total protein, according to the rate of formation of glyoxylate phenylhydrazone in the presence of isocitrate and phenylhydrazine at room temperature as described previously (31, 32). One unit of enzyme activity corresponds to the production of 1 μmol of glyoxylate phenylhydrazone per minute under assay conditions.

Promoter activity assay

Promoter activity was measured by monitoring proline iminopeptidase (PIP) activity as the reporter, as described previously (19). Various lengths of the upstream region of icl_{Re} were amplified using Pfu Turbo DNA polymerase (Stratagene, La Jolla, CA). First, the PCR fragment that was amplified by using the primers icl-303 (5′-CGCTGTACAGCGAACTGCCGGAATTTGCAAGTG -3′; *Bsr*GI site is underlined) and icl-1 (5′-CATGCCATGGCCAAGACTCCATCTCTTTGATCTGC -3′; *Nco*I site is underlined) was inserted into pHN409 (20) digested with *Bsr*GI and *Nco*I, yielding p303-QC1-PIP. For the deletion series, 8 lengths of the upstream region of icl_{Re} were amplified using 8 pairs of primers as follows: for -202 bp, icl-202 (5′-AATGTACATACCAGCCGTGTAGGA-3′) and pip-AS (5′-GGTCG*ACTAGT*TTATTAATGATGA-3′); -192 bp, icl-192 (5′-AATGTACAGTAGGAATCTTCACAG-3′) and pip-AS; -182 bp, icl-182 (5′-AATGTACATCACAGACTTAGCAAA-3′) and pip-AS; -172 bp, icl-172

(5′-AATGTACAAGCAAAGTGTGTTGAA-3′) and pip-AS; -152 bp, icl-152 (5′-AATGTACATAGCGAAGATTGGCAT-3′) and pip-AS; -102 bp, icl-102 (5′-AATGTACAATTCTCGGTAAGTACA-3′) and pip-AS; -75 bp, icl-75 (5′-AATGTACATGGCAAGTATGTGAAG-3′) and pip-AS; and -52 bp, icl-52 (5′-AATGTACACACGTACTGCTCACAA-3′) and pip-AS. *Bsr*GI and *Spe*I sites are underlined and italicized, respectively. Each PCR product was inserted into p303-QC1-PIP digested with *Bsr*GI and *Spe*I, yielding p202-QC1-PIP, p192-QC1-PIP, p182-QC1-PIP, p172-QC1-PIP, p152-QC1-PIP, p102-QC1-PIP, p75-QC1-PIP, and p52-QC1-PIP, respectively. PCR was performed with Pfu turbo DNA polymerase. Cells harboring these plasmids were cultured according to the method used for the preparation of total protein, and total protein that was obtained from 20 mL culture was subjected to PIP activity analysis.

Isolation of proteins that were bound to the upstream region of icl_{Re}

The upstream region of icl_{Re} was amplified using a sense primer, icl-201 (5′-ACCAGCCGTGTAGGAATCTTCACAG-3′), and a biotin-labeled antisense primer, icl-1+B (5′-CAAGACTCCATCTCTTTGATCTGCT-3′). The biotin-labeled DNA fragment (50 pmol) was mixed with 200 μL of streptavidin-coated magnet beads (Invitrogen) containing 30 mg total protein from *R. erythropolis* PR4, which was prepared in the presence of 5 mM EDTA and concentrated with Amicon Ultra-10,000 NMWL (Millipore, Bedford, MA). The mixture was incubated for 30 min at room temperature. Then, the magnet beads were washed with TE buffer 4 times and were

boiled in loading buffer containing SDS, followed by SDS-PAGE analysis. Then, the protein band was excised and subjected to LC-MS/MS analysis as previously described.

Pull-down analysis of $RamB_{Re}$ by using the upstream region of icl_{Re}

For the pull-down analysis of $RamB_{Re}$, 1.5 mg total protein, which was obtained from cells expressing recombinant $RamB_{Re}$, and 25 pmol biotin-labeled DNA fragments were used. Expression of recombinant $RamB_{Re}$ was performed as follows: first, the PCR fragment was amplified using the primers DBP-Nterm (5′-GGAATTCCATATGTCGAAAACCTTTGTCGGTGTCC-3′; *Nde*I site is underlined) and DBP-Cterm (5′-CGGGATCCTCAGCGAATCACGTAAGGCGAAATC-3′; *Hin*dIII site is underlined), and was inserted into pTip-QC2 (20) digested with *Nde*I and *Hin*dIII, yielding pTip-QC2-DBP. Expression of $RamB_{Re}$ was performed using *R. erythropolis* JCM3201 harboring pTip-QC2-DBP in the presence of 0.5 μg/μL thiostrepton as an inducer. Various lengths of the upstream region of icl_{Re} were amplified using the following primers corresponding to the fragments illustrated in Fig. 4B. For fragment e, icl-201; d, icl-151 (5′-AGCGAAGATTGGCATTAGCAACAGG-3′); c, icl-101 (5′-TTCTCGGTAAGTACACAAGAAGGGC-3′); b, icl-76 (5′-CTGGCAAGTATGTGAAGTAGTACGCA-3′); a, icl-61 (5′-AGTAGTACGCACGTACTGCTCACAA-3′). Each primer was used in combination with icl-1+B. For fragments f and g, p303(61-76KO)-QC1-PIP, which has a gap between the -76 and -61 bp region of p303-QC1-PIP, was used as template. Then,

PCR was performed using the following primers: for f, icl-127 (5′-GTAGACGGCACTTTTTCGATGTGCC-3′); g, icl-142 (5′-TGGCATTAGCAACAGGTAGACGGCA-3′). Each primer was used in combination with icl-1+B. p303(61-76KO)-QC1-PIP was constructed by inverse PCR with the primers 61-76KO_S (5′-TAGTACGCACGTACTGCTCACAACAGGCC-3′) and 61-76KO_AS (5′-GGCCCTTCTTGTGTACTTACCGAGAATGG-3′). PCR was performed with Pfu turbo DNA polymerase.

Construction of a ramB_{Re} *knockout mutant*

To construct an *R. erythropolis* PR4 $ramB_{Re}$ knockout mutant, a partial region of $ramB_{Re}$, which was amplified using the primers DBPKO-S (5′-GGGGTACCGAGATCGCCAGACGCCTCGA-3′; *Kpn*I site is underlined) and DBPKO-AS (5′-GCTCTAGAACCGGATATGAGAACGTCTCG-3′; *Xba*I site is underlined), was subcloned in pHN267 (20). The vector containing the partial region of $ramB_{Re}$ was introduced into wild-type *R. erythropolis* PR4 by electroporation. One hundred transformants were subjected to colony PCR, and 2 of them were confirmed to harbor the gene disruption intended.

Construction of expression vectors, and cloning of pip *and* vdh *(vitamin* D_3 *hydroxylase)*

The 303-bp (P_{icl}), 102-bp (P_{cpi}, constitutive promoter region of icl_{Re}) upstream region

304 of icl_{Re} were amplified using specific primers, as described previously. These DNA
305 fragments were inserted into pNit-QC1, pNit-QC2, pNit-QT1, pNit-QT2, pNit-RC1,
306 pNit-RC2, pNit-RT1, pNit-RT2 (20) digested with *Bsr*GI and *Nco*I, yielding 16 types
307 novel expression vectors, pIcl (or pCpi)-QC1, pIcl (or pCpi)-QC2, pIcl (or pCpi)-QT1,
308 pIcl (or pCpi)-QT2, pIcl (or pCpi)-RC1, pIcl (or pCpi)-RC2, pIcl (or pCpi)-RT1, pIcl
309 (or pCpi)-RT2, respectively (Fig. S1-A).
310 The *vdh* fragment was isolated by pET29-VDH (26) digested *Nde*I and *Xho*I, and
311 was cloned into *Nde*I/*Xho*I sites of pIcl-QC2 or pCpi-QC2, yielding pIcl-QC2-VDH and
312 pCpi-QC2-VDH, respectively. Those vectors were transformed into *R. erythropolis*
313 JCM 3201 wild-type cells by electroporation as described previously (23).
314 pIcl-QC1-PIP and pCpi-QC1-PIP, which are identical to p303-QC1-PIP and
315 p102-QC1-PIP, respectively, were used for PIP expression.
316
317 **Results**
318
319 *Protein expression changes in the presence of organic solvents*
320
321 To select which organic solvent can be a candidate as an inducer of protein
322 expression, we used 11 different organic solvents as described in Materials and Methods.
323 As host cells, we randomly selected 4 strains of *R. erythropolis* from our laboratory
324 collections. *R. erythropolis* NI86/21, JCM6824, JCM3201, and PR4 were grown to a
325 stationary phase and a part of the culture was added to fresh media containing either 1%
326 or 5% of the above-mentioned organic solvents. Although all 4 strains were tolerant to
327 most of these solvents even at 5% concentration, none of the strains grew in the

328 presence of 5% 1-butanol (data not shown).

329 Total proteins from cells grown either in the presence or absence of organic solvents
330 were separated using SDS-PAGE. While the protein band patterns were not affected by
331 the organic solvents other than methanol, the amount of the ~46-kDa band was
332 increased by methanol in all strains examined (Fig. 1A and data not shown). The
333 amount of proteins increased was highest in the strain PR4. The induction of ~46-kDa
334 proteins reached almost 80% of its maximum level within 6 h, and it gradually
335 increased until 24 h after the addition of methanol (Fig. 1B). The ~46-kDa band was
336 also induced in the presence of 1% methanol (data not shown).

337

338 *Identification of 46-kDa proteins induced in the presence of methanol and gene*
339 *cloning*

340

341 Since the ~46-kDa band was close to other bands on the acrylamide gel, we
342 performed further separation . Briefly, total proteins that were obtained from the cells
343 grown either in the presence or absence of methanol were subjected to size exclusion
344 column chromatography, and the fractions that contained proteins of around 46 kDa
345 were pooled and separated by 2-DE. By comparing the 2-DE spot patterns between
346 those 2 samples, we found a spot that was observed only in the 2-DE sample obtained
347 from cells grown in the presence of methanol (Fig. 1C). The spot was excised from the
348 acrylamide gel followed by trypsin digestion and was subjected to MS analysis. Three
349 amino acid sequences were obtained (VLIPTQQHIR, TDAEAATLITSDVDER, and
350 LASDVADVPSVIIAR) and were similar to ICL of *Rhodococcus equi*, *Rhodococcus*
351 *fascians*, and *Corynebacterium efficiens*, and elongation factor Tu (EF-Tu) of

352 *Mycobacterium tuberculosis* and *Lactobacillus sakei*, respectively. Since the molecular
353 weight of EF-Tu should be smaller than that estimated by the 2-DE, it seemed to be a
354 contaminated protein.
355 To identify the gene encoding for ICL_{Re}, we performed inverse PCR by using
356 degenerate primers as described in Materials and Methods. By inverse PCR, we
357 obtained 2 different DNA fragments from genome fragments that were digested with
358 either *Nco*I or *Bam*HI (Fig. 2A). These fragments covered an approximately 11-kbp
359 DNA sequence including icl_{Re}, corresponding to *R. erythropolis* PR4 chromosome
360 1710445-1721421, and gene bank accession number is NC_012490. DNA sequencing
361 identified 8 open reading frames (ORFs), and 4 consecutive ORFs were found in the
362 same direction. These 4 ORFs started with icl_{Re} followed by 3-hydroxyacyl-CoA
363 dehydrogenase (*hbd*), 5-methyltetrahydropteroyltriglutamate-homocysteine
364 *S*-methyltransferase (*mhm*), and alcohol dehydrogenase (*adh*). Genome information of
365 *R. erythropolis* PR4 is currently available, and the accession numbers for these genes
366 are as follows: icl_{Re}, RER_15740; *hbd*, RER_15750; *mhm*, RER_15760, and *adh*,
367 RER_15770. To investigate if these 4 ORFs are polycistronically transcribed, we
368 performed RT-PCR analysis with specific primers that were designed to amplify DNA
369 fragments containing more than 2 consecutive ORFs (Fig. 2B). We detected RT-PCR
370 products when using 5 different primer sets as shown in Fig. 2B, although DNA
371 fragments containing all of the 4 ORFs were not amplified, probably because RT
372 reaction is difficult for long mRNAs.
373
374 *Promoter activity assay with the 5′ upstream region of* icl_{Re}
375

376 The promoter activity of the upstream region of *icl*$_{Re}$ was analyzed using *pip* as a
377 reporter gene. Different lengths of the upstream region of *icl*$_{Re}$ were connected to *pip*,
378 and the protein amount and enzymatic activity of PIP were monitored before and after
379 the addition of methanol (Fig. 3A). When the 303-bp upstream region of *icl*$_{Re}$ was used,
380 the protein amount and enzymatic activity were bothinduced by methanol in a
381 time-dependent manner. The induction profile of PIP was similar to that of ICL$_{Re}$.
382 To find the minimal promoter region, we constructed different sizes of the upstream
383 region of *icl*$_{Re}$ connected to *pip* (Fig. 3B). A similar response was observed for the 303-
384 and 202-bp upstream regions of *icl*$_{Re}$, and PIP activity was induced in a time-dependent
385 manner. Shortening the length of the upstream region decreased the inducibility and
386 expression level, except for the 2 constructs containing the -152-bp and -102-bp
387 upstream regions. In these cases, the expression levels were high even in the absence of
388 methanol. The expression level of the -102-bp upstream region was 1.8 times higher
389 than that observed for the methanol-inducible promoter.
390
391 *Isolation of proteins that were bound to the putative promoter region of* icl$_{Re}$
392
393 To identify regulatory factors for *icl*$_{Re}$ expression, pull-down analysis with the
394 biotin-labeled upstream region of *icl*$_{Re}$ was performed as described in Materials and
395 Methods. Proteins that were bound to the biotin-labeled DNA fragments were collected
396 using streptavidin-coated magnet beads and were analyzed by SDS-PAGE (data not
397 shown), which detected 2 major bands (~53 and ~65 kDa). Since the ~65-kDa band was
398 also detected in the negative control experiment in which the total protein was incubated
399 with only streptavidin beads, we focused on only the ~53-kDa protein for the further

400 analysis.

401 To identify the ~53-kDa protein, LC-MS/MS analysis was performed. A database
402 search matched peptide sequences that were deduced from the MS analysis to some
403 different protein sequences, including the RamB homologue from *Rhodococcus jostii*
404 RHA1 and *Mycobacterium smegmatis*, and acyl-coenzyme A carboxylase from
405 *Corynebacterium diphtheriae*. We chose only $RamB_{Re}$ for the further analysis, because
406 the other proteins were not putative transcriptional regulators. RamB from
407 *Corynebacterium glutamicum* ($RamB_{Cg}$) is a transcriptional regulator and negatively
408 controls the expression of some genes, including *icl* (33).

409 In the case of *C. glutamicum*, the 13-bp binding motif for $RamB_{Cg}$
410 (5′-AA/GAACTTTGCAAA-3′) is identified in the upstream region of icl_{Cg}. However,
411 homologous sequence was not found in the upstream region of icl_{Re}. Therefore, we
412 confirmed the binding ability of $RamB_{Re}$ to the upstream region of icl_{Re} by pull-down
413 experiments; the biotin-labeled upstream region of icl_{Re} was mixed with the total
414 proteins obtained from *R. erythropolis* PR4 cells expressing recombinant $RamB_{Re}$ (Fig.
415 4C). By the experiments, at least 2 possible binding sites were found: one is located
416 between -61 and -76 bp (5′-TGGCAAGTATGTGAAG-3′) and the other is located
417 between -127 and -142 bp (5′-TGGCATTAGCAACAGG-3′) (Fig. 4A).

418

419 *Effect of* $ramB_{Re}$ *disruption on* R. erythropolis *PR4*

420

421 The above pull-down experiments suggested that $ramB_{Re}$ was involved in the
422 regulation of icl_{Re} expression. To investigate the role of $RamB_{Re}$ in icl_{Re} expression, we
423 analyzed the ICL_{Re} activity of wild-type and $ramB_{Re}$ knockout mutant in the presence of

various carbon sources (Table 1). Gene knockout was done by a single crossover homologous recombination. Since random recombination of exogenous DNA fragments often occurs in *R. erythropolis*, we checked the candidate clones in the gene arrangement around $ramB_{Re}$ by using PCR, and obtained a knockout mutant (data not shown).

In *C. glutamicum* and *M. tuberculosis*, it has been reported that the expression of *icl* is negatively regulated by RamB and is dependent on the carbon source availability in the culture media (33-37). In wild-type *R. erythropolis* PR4, ICL_{Re} activity was induced in the presence of methanol and acetate, while these inductions were suppressed by the addition of glucose. In contrast, in the knockout mutant, we did not observe a significant difference among them.

Expression vector construction by using the promoter from the 5' upstream region of icl_{Re}

Since the activity of the 303-bp upstream region of icl_{Re} was methanol inducible and that of the 102-bp upstream region was constitutively very high, we believe they could be used as a methanol-inducible and strong constitutive promoter for recombinant protein expression, respectively. We have recently cloned antibiotic resistance genes, 2 different types of replication origins, and constitutive or inducible promoters from the genus *Rhodococcus* (19, 20). By using these elements, we have constructed a wide variety of expression vectors. Here, we combined these elements with the promoter region of icl_{Re}, and constructed constitutive or methanol-inducible expression vectors (representative constructs are shown in Fig. 5A). One of the promoters was P_{icl} ,which

448 includes the 303-bp upstream region of icl_{Re}, and another one was P_{cpi} (constitutive
449 promoter region of icl_{Re}), which includes the 102-bp upstream region of icl_{Re}. By
450 combining 2 types of selection markers, replication origins, and multiple-cloning sites
451 as described previously (20), we constructed 16 types of vectors (Fig. S1). In order to
452 test the expression ability of these expression vectors, PIP and VDH were expressed as
453 model cases. When P_{icl} was used for the expression, protein expression was inducible
454 depending on the presence of methanol, and when P_{cpi} was used, constitutive high
455 expression was observed in both cases of PIP and VDH (Fig. 5B). As shown in Figure
456 5C, the expression level of P_{cpi} was quite high and its activity exhibited approximately
457 3- and 2-fold higher than P_{icl} and P_{tip}, respectively.
458
459 **Discussion**
460
461 All of the *R. erythropolis* strains used in this study exhibited tolerance to various
462 kinds of organic solvents at certain concentrations, and all strains tested grew in the
463 presence of 5% methanol. By analyzing cell responses to organic solvents through
464 SDS-PAGE, we found a protein that was induced in the presence of methanol. The
465 protein was identified as ICL_{Re} by LC-MS/MS analysis, and its methanol-inducible
466 regulation was revealed to depend on the at least 200-bp upstream region of icl_{Re}. We
467 also found $ramB_{Re}$ as one of the regulatory factors of icl_{Re} expression.
468 RT-PCR data suggested that icl_{Re} would be cotranscribed with 3 other neighboring
469 genes. Thus, it would be reasonable to think that the other 3 proteins would also be
470 induced in the presence of methanol. However, in this study, only ICL_{Re} was found to be
471 induced in the presence of methanol by using acrylamide gels and 2-DE. This may be

472 due to the differences in protein turnover rate among these proteins or the differences in
473 translation rate of mRNA even in a single cistron.
474 ICL is a key enzyme in the glyoxylate cycle and is essential for the shunt pathway
475 of the TCA cycle. ICL is induced in the presence of acetate in *Corynebacterium* and
476 *Mycobacterium* (35, 38, 39). In *R. erythropolis* PR4, ICL_{Re} was induced by the addition
477 of sodium acetate, suggesting a similar regulation of icl_{Re} expression as that of
478 *Corynebacterium* or *Mycobacterium*. Also, $ramB_{Re}$ knockout experiment supports the
479 idea that $RamB_{Re}$ functions as a suppressor of icl_{Re}.
480 In the analysis of the minimal promoter of icl_{Re}, reporter expression was gradually
481 decreased in both of the methanol-inducibility and the amount of protein expression as
482 the upstream region used was shortened, except for constructs containing the -152 and
483 -102 bp upstream regions. This would suggest that there are at least 2 different
484 regulation mechanisms: one involves positive regulation, the function of which depends
485 on the length of the upstream region, and the other involves negative regulation, the
486 function of which depends on the region between -152 and -102 bp. The expression
487 would be regulated not only by $RamB_{Re}$, as described below, but also by another factor
488 that would regulate the expression by interacting with the upstream region of icl_{Re}
489 between -152 and -102 bp. The details of the regulation mechanism(s) of icl_{Re} by
490 $RamB_{Re}$ in *R. erythropolis* remain to be elucidated.
491 By using various lengths of the biotin-labeled upstream region of icl_{Re}, we identified
492 2 possible binding sites of $RamB_{Re}$. However, we could not find any sequence similarity
493 between these 2 sites, and neither of these sequences contained the core motif of *C.*
494 *glutamicum* RamB binding sites, 5′-TTTGCAAA-3′ (36). As shown in Fig. 4, the
495 amount of $RamB_{Re}$ binding to the upstream region of icl_{Re} was apparently different

among the 101-, 151-, and 201-bp upstream regions. The amount of binding protein seems higher for the longer regions, suggesting there would be at least 3 binding sites, which would be located between -61 and -101 bp, -101 and -151 bp, and -151 and-201 bp, respectively. Although we did not obtain experimental data, we found a sequence similar to that between -142 and -127 bp in the region between -101 and -151 bp (Fig. 4D). This sequence was located between -179 and -164 bp (5′-CAGACTTAGCAAAGTG-3′). Also, these 2 sites contain 5′-TTAGCAA-3′, which is similar to the core-binding motif of $RamB_{Cg}$, suggesting a possibility of $RamB_{Re}$ binding to this region. $RamB_{Re}$ has 2 functional domains, the helix turn helix (HTH) motif and transcriptional regulation domains (Fig. S2). Since the HTH motif, which is important for recognizing the target binding sequence, was not highly conserved among related genera, the relation between the HTH motif and RamB binding sequence remains to be elucidated. Also, the genome structure around *icl* is highly diverse among related genera (Fig. S3). This diversity would be related to the regulation difference of *icl* among related genera.

The response to solvent stress has not been well understood, although *R. erythropolis* is often said to be tolerant to organic solvents. The general mechanism of solvent tolerance has been reported to include rigidification of the cell membrane, change in the membrane's protein content or composition, active export of solvent, adaptation of energetic status, changes in cell wall and outer membrane composition, modification of cell surface properties, morphological changes, and metabolism or transformation of the solvent (11). In the case of *R. erythropolis* PR4 methanol tolerance, assimilation of methanol would be related to the mechanism because the shunt pathway of the TCA cycle, which is also needed for C1 carbon assimilation,

would be activated in the presence of methanol. To investigate this possibility, we performed 2 preliminary experiments: one was HPLC measurement of the amount of methanol before and after the incubation of *R. erythropolis* PR4, and the other was observation of growth of *R. erythropolis* PR4 in minimal media containing methanol as a sole carbon and energy source. However, neither of these experiments supported the possibility (data not shown). These data suggest that icl_{Re} regulation by methanol would be different from what is done by acetate through glyoxylate cycle. This would be supported by the difference of *icl* response to actetate or methanol in the presence of glucose (Table1).

Methanol-inducible promoters have been identified from methanol-assimilating bacteria such as *Methylobacterium extorquens* and *Candida boidinii* (40-42). However, such promoters were never applied to create expression vectors. Although functional analysis of icl_{Re} induction has not been completed, the novel vectors described here would be useful for bioreactions.

Acknowledgments

We thank all the members of our laboratory for their help and discussion. The genome information of *R. erythropolis* PR4 was kindly provided by NITE. This work was supported in part by the Project on Development of Technology for High-efficiency Conversion of Biomass and Other Energy by the New Energy and Industrial Technology Development Organization (NEDO).

References

1. **Finnerty, W. R.:** The biology and genetics of the genus *Rhodococcus*, Annu. Rev. Microbiol., **46**, 193-218 (1992).
2. **Bell, S. K., Philp, C. J., Aw, J. D. W., and Christofi, N.:** The genus *Rhodococcus*, J. Appl. Microbiol., **85**, 195-210 (1998).
3. **Larkin, J. M., De Mot, R., Kulakov, A. L., and Nagy, I.:** Applied aspects of *Rhodococcus* genetics, Antonie Leeuwenhoek, **74**, 133-153 (1998).
4. **Van der Geize, R., and Dijkhuizen, L.:** Harnessing the catabolic diversity of rhodococci for environmental and biotechnological applications, Curr. Opin. Microbiol., **7**, 255-261 (2004).
5. **Warhurst, A. M., and Fewson, C. A.:** Biotransformations catalyzed by the genus *Rhodococcus*, Crit. Rev. Biotechnol., **14**, 29-73 (1994).
6. **Walter, U., Beyer, M., Klein, J., and Rehm, J. H.:** Degradation of pyrene by *Rhodococcus* sp. UW1, Appl. Microbiol. Biotechnol., **34**, 671-676 (1991).
7. **Paje, L. M., Neilan, A. B., and Couperwhite, I.:** A *Rhodococcus* species that thrives on medium saturated with liquid benzene, Microbiol., **143**, 2975-2981 (1997).
8. **Na, K. S., Kuroda, A., Takiguchi, N., Ikeda, T., Ohtake, H., and Kato, J.:** Isolation and characterization of benzene-tolerant *Rhodococcus opacus* strains, J. Biosci. Bioeng., **99**, 378-382 (2005).
9. **Peng, X., Taki, H., Komukai, S., Sekine, M., Kanoh, K., Kasai, H., Choi, S. K., Omata, S., Tanikawa, S., Harayama, S., and Misawa, N.:** Characterization of four *Rhodococcus* alcohol dehydrogenase genes responsible for the oxidation of

568 aromatic alcohols, Appl. Microbiol. Biotechnol., **71**, 824–832 (2006).
569 10. **León, R., Fernandes, P., Pinherio, H. M., and Cabral, J. M. S.:** Whole-cell
570 biocatalysis in organic media, Enzyme Microb. Technol., **23**, 483-500 (1998).
571 11. **Heipieper, J. H., Neumann, G., Cornelissen, S., and Meinhardt, F.:**
572 Solvent-tolerant bacteria for biotransformations in two-phase fermentation systems,
573 Appl. Microbiol. Biotechnol., **74**, 961-973 (2007).
574 12. **Verhoef, S., Wierckx, N., Westerhof, M. G. R., de Winde, H. J., and**
575 **Ruijssenaars, J. H.:** Bioproduction of *p*-hydroxystyrene from glucose by the
576 solvent-tolerant bacterium *Pseudomonas putida* S12 in a two-phase water-decanol
577 fermentation, Appl. Env. Microbiol., **75**, 931-936 (2009).
578 13. **De Bont, J. A. M.:** Solvent-tolerant bacteria in biocatalysis. Trends Biotechnol.,
579 **16**, 493-499 (1998).
580 14. **Nicolaou, S. A., Gaida, S. M., and Papoutsakis, E. T.:** A comparative view of
581 metabolite and substrate stress and tolerance in microbial bioprocessing: from
582 biofuels and chemicals, to biocatalysis and bioremediation, Metab. Eng., **12**,
583 307-331 (2010).
584 15. **Favre-Bulle, O., Schouten, T., Kingma, J., and Witholt, B.:** Bioconversion of
585 n-octane to octanoic acid by a recombinant *Escherichia coli* cultured in a
586 two-liquid phase bioreactor, Bio/technology, **9**, 367-371 (1991).
587 16. **Kobayashi, H., Yamamoto, M., and Aono, R.:** Appearance of a stress-response
588 protein, phage-shock protein A, in *Escherichia coli* exposed to hydrophobic
589 organic solvents, Microbiol., **144**, 353-359 (1998).
590 17. **Aono, R.:** Improvement of organic solvent tolerance level of *Escherichia coli* by
591 overexpression of stress-responsive genes, Extremophiles, **2**, 239-248 (1998).

18. **Aono, R., and Kobayashi, H.:** Cell surface properties of organic solvent-tolerant mutants of *Escherichia coli* K-12, Appl. Microbiol. Biotechnol., **63**, 3637-3642 (1997).

19. **Nakashima, N., and Tamura, T.:** A novel system for expressing recombinant proteins over a wide temperature range from 4 to 35 ˚C, Biotechnol. Bioeng., **86**, 136-148 (2004).

20. **Nakashima, N., and Tamura, T.:** Isolation and characterization of a rolling-circle-type plasmid from *Rhodococcus erythropolis* and application of the plasmid to multiple-recombinant-protein expression, Appl. Environ. Microbiol., **70**, 5557-5568 (2004).

21. **Mitani, Y., Meng, X. Y., Kamagata, Y., and Tamura, T.:** Characterization of LtsA from *Rhodococcus erythropolis* , an enzyme with glutamine amidotransferase activity, J. Bacteriol., **187**, 2582–2591 (2005).

22. **Mitani, Y., Nakashima, N., Sallam, I. K., Toriyabe, T., Kondo, K., and Tamura, T.:** Advances in the development of genetic tools for the genus *Rhodococcus*, Actinomycetologica, **20**, 55-61 (2006).

23. **Sallam, K. I., Mitani, Y., and Tamura, T.:** Construction of random transposition mutagenesis system in *Rhodococcus erythropolis* using IS*1415*, J. Biotechnol., **121**, 13-22 (2006).

24. **Sallam, K. I., Tamura, N., and Tamura, T.:** A multipurpose transposon-based vector system mediates protein expression in *Rhodococcus erythropolis*, Gene, **386**, 173-182 (2007).

25. **Sallam, K. I., Tamura, N., Imoto, N., and Tamura, T.:** New vector system for random, single-step integration of multiple copies of DNA into the *Rhodococcus*

genome, Appl. Environ. Microbiol., **76**, 2531-2539 (2010).

26. **Fujii, Y., Kabumoto, H., Nishimura, K., Fujii, T., Yanai, S., Takeda, K., Tamura, N., Arisawa, A., and Tamura, T.:** Purification, characterization, and directed evolution study of a vitamin D_3 hydroxylase from *Pseudonocardia autotrophica*, Biochem. Biophys. Res. Comm., **385**, 170-175 (2009).

27. **Imoto, N., Nishioka, T., and Tamura, T.:** Permeabilization induced by lipid II-targeting lantibiotic nisin and its effect on the bioconversion of vitamin D_3 to 25-hydroxyvitamin D_3 by *Rhodococcus erythropolis*, Biochem. Biophys. Res. Comm., **405**, 393-398 (2011).

28. **Rosenfeld, J., Capdevielle, J., Guillemot, J. C., and Ferrara, P.:** In-gel digestion of proteins for internal sequence analysis after one-or two-dimensional gel electrophoresis, Anal. Biochem., **203**, 173-179 (1992).

29. **Hellman, U., Wernstedt, C., Góñez, J., and Heldin, C. H.:** Improvement of an "In-gel" digestion procedure for the micropreparation of internal protein fragments for amino acid sequencing, Anal. Biochem., **224**, 451-455 (1995).

30. **Sun, N., Tamura, N., Tamura, T., Knispel, R. W., Hrabe, T., Kofler, C., Nickell, S., and Nagy, I.:** Size distribution of native cytosolic proteins of *Thermoplasma acidophilum*, Proteomics, **9**, 3783-3786 (2009).

31. **Serrano, A. J., Camacho, M., and Bonete, J. M.:** Operation of glyoxylate cycle in halophilic archaea: presence of malate synthase and isocitrate lyase in *Haloferax volcanii*, FEBS letter, **434**, 13-16 (1998).

32. **Wall, M. D., Duffy, S. P., DuPont, C., Prescott, F. J., and Meijer, G. W.:** Isocitrate lyase activity is required for virulence of the intracellular pathogen *Rhodococcus equi*, Infect. Immun., **73**, 6736-6741 (2005).

33. **Wendisch, V. F., Spies, M., Reinscheid, D. J., Schnicke, S., Sahm, H., and Eiksmanns, B. J.:** Regulation of acetate metabolism in *Corynebacterium glutamicum*: transcriptional control of the isocitrate lyase and malate synthase genes, Arch. Microbiol., **168**, 262-269 (1997).

34. **McKinney, J. D., Höner zu Bentrup, K., Muñoz-Elías, E. J., Miczak, A., Chen, B., Chan, W. T., Swenson, D., Sacchettini, J. C., Jacobs, W. R. Jr., and Russell, D. G.:** Persistence of *Mycobacterium tuberculosis* in macrophages and mice requires the glyoxylate shunt enzyme isocitorate lyase, Nature, **406**, 735-738 (2000).

35. **Micklinghoff, J. C., Breitinger, K. J., Schmidt, M., Geffers, R., Eikmanns, B. J., and Bange, F. C.:** Role of the transcriptional regulator RamB (Rv0465c) in the control of the glyoxylate cycle in *Mycobacterium tuberculosis*, J. Bacteriol., **23**, 7260-7269 (2009).

36. **Auchter, M., Cramer, A., Hüser, A., Rückert, C., Emer, D., Schwarz, P., Arndt, A., Lange, C., Kalinowski, J., Wendisch, V. F., and Eikmanns, B. J.:** RamA and RamB are global transcriptional regulators in *Corynebacterium glutamicum* and control genes for enzymes of the central metabolism, J. biotechnol., **154**, 126-139 (2011).

37. **Teramoto, H., Inui, M., and Yukawa, H.:** Transcriptional regulators of multiple genes involved in carbon metabolism in *Corynebacterium glutamicum*, J. Biotechnol., **154**, 114-125 (2011).

38. **Gerstmeir, R., Cramer, A., Dangel, P., Schaffer, S., and Eikmanns, B. J.:** RamB, a novel transcriptional regulator of genes involved in acetate metabolism of *Corynebacterium glutamicum*, J. Bacteriol., **186**, 2798-2809 (2004).

39. **Höner zu Bentrup, K., Miczak, A., Swenson, D. L., and Russell, D. G.:** Characterization of activity and expression of isocitrate lyase in *Mycobacterium avium* and *Mycobacterium tuberculosis*, J. Bacteriol., **181**, 7161-7167 (1999).

40. **Morris, C. J., and Lidstrom, M. E.:** Cloning of a methanol-inducible *moxF* promoter and its analysis in *moxB* mutants of *Methylobacterium extorquens* AM1rif, J. Bacteriol., **174**, 4444-4449 (1992).

41. **Yukimoto, H., Komeda, T., Lim, R. C., Nakagawa, T., Kondo, K., Kato, N., and Sakai, Y.:** Regulation and evaluation of five methanol-inducible promoters in the methylotrophic yeast *Candida boidinii*, Biochim. Biophys. Acta, **1493**, 56-63 (2000).

42. **Choi, Y. J., Morel, L., Bourque, D., Mullick, A., Massie, B., and Míguez, C. B.:** Bestowing inducibility on the cloned methanol dehydrogenase promoter (P_{mxaF}) of *Methylobacterium extorquens* by applying regulatory elements of *Pseudomonas putida* F1, Appl. Environ. Microbiol., **72**, 7723-7729 (2006).

682 **Figure legends**

683

684 Fig. 1. SDS-PAGE and 2-DE analyses of the total protein of *Rhodococcus erythropolis*
685 PR4 incubated either in the presence or absence of methanol. (A) Total proteins were
686 extracted from PR4 cells grown for 24 h either in the presence or absence of 5%
687 methanol, and 15 μg protein was separated on an acrylamide gel. The arrowhead
688 indicates proteins induced by the addition of 5% methanol. Lanes – and +, total protein
689 obtained from cells grown in the absence and presence of 5% methanol, respectively.
690 (B) A time course analysis of the ~46-kDa protein was performed using 15%
691 acrylamide gel. Fifteen micrograms of total protein was subjected to SDS-PAGE
692 analysis. The arrowhead indicates proteins that were induced by the addition of 5%
693 methanol. Lane numbers indicate the incubation time after the addition of 5% methanol.
694 (C) 2-DE analysis of the total proteins. The arrow indicates proteins that were induced
695 by 5% methanol.

696

697 Fig. 2. A 11-kbp *R. erythropolis* PR4 DNA fragment including a probable icl_{Re} operon.
698 (A) Schematic drawing made using the sequence analysis data obtained by inverse PCR.
699 The recognition sites of restriction enzymes used for the inverse PCR are indicated
700 above the drawing. The direction of the open arrow indicates the direction of each ORF.
701 *ramB*, transcriptional regulator of acetate metabolism; *aad*, acetamidase; *prp*, putative
702 regulatory protein; *icl*, isocitrate lyase; *hbd*, 3-hydroxyacyl-CoA dehydrogenase; *mhm*,
703 5-methyltetrahydropteroyltriglutamate-homocysteine *S*-methyltransferase; *adh*, alcohol
704 dehydrogenase. The accession numbers for these genes are as follows: *ramB*,
705 RER_15700; *aad*, RER_15710; *prp*, RER_15720. The white arrow indicates

706 hypothetical protein; the gray arrows indicate 4 ORFs of probable polycistron. (B)
707 RT-PCR was performed using 1 μg of total RNA as a starting material, and the PCR
708 product was subjected to electrophoresis using 1% agarose gel (left). Lanes “a” to “e”
709 correspond to the gene fragment that is indicated on the right side of the panel.
710
711 Fig. 3. Promoter activity analysis by using deletion series of the upstream region of icl_{Re}
712 and time course analysis. (A) Promoter activity analysis of the 303-bp upstream region
713 of icl_{Re}. SDS-PAGE was performed using 15 μg of total protein from PR4 cells
714 expressing PIP. The arrowhead indicates PIP. The specific activity of PIP was
715 colorimetrically measured using proline-7-amino-4-methylcoumarin as a substrate. (B)
716 PIP activity in *R. erythropolis* PR4 cells carrying plasmids with various deletions of the
717 upstream region of icl_{Re} were measured. The cells were incubated in the presence of 5%
718 methanol for 0, 2, and 8 h, and subjected to PIP activity assay.
719
720 Fig. 4. *Cis*-element analysis of the icl_{Re} promoter region. (A) Schematic drawing of the
721 *icl* promoter region containing putative *cis* elements. The *cis* elements that were
722 identified by the binding assays are indicated by 2 black boxes, while a probable *cis*
723 element that was deduced from the sequence similarity is indicated by an open box.
724 Nucleotide positions were calculated from the first base of translation initiation codon
725 (ATG, +1). (B) DNA fragments used for the pull-down analysis are schematically
726 illustrated. (C) The protein that was bound to the DNA fragment was analyzed on an
727 acrylamide gel. The lane names correspond to the construct names. The arrowhead
728 indicates $RamB_{Re}$. (D) Alignment of the sequence of $RamB_{Re}$ binding sites in the
729 upstream of icl_{Re} -61 to -76 bp, -127 to -142 bp, and -164 to -179 bp. Boxed sequences

730 (black) represent the identities of at least 2 members of the group.

731

732 Fig. 5. Expression vector construction and application by using the promoter from the
733 upstream region of icl_{Re}. (A) Schematic map of pIcl-QC1 and pCpi-QC1. cm^r,
734 chloramphenicol-resistant gene; amp^r, ampicillin-resistant gene; *Col*E1, replication
735 origin for *E. coli*; T_{thcA}, *thcA* transcriptional terminator; MCS, multiple-cloning site; P_{icl},
736 303-bp upstream region of icl_{Re} (methanol-inducible promoter); P_{cpi}, 102-bp upstream
737 region of icl_{Re} (constitutive strong promoter); *repAB*, essential region for stable
738 maintenance of the plasmid in *R. erythropolis*. (B) (Left) Expression profiles of PIP or
739 VDH in *R. erythropolis* JCM3201 containing the pIcl-QC1-PIP or pIcl-QC2-VDH,
740 respectively. Total proteins (15 μg) were analyzed by SDS-PAGE. Black and gray
741 arrowheads indicate PIP and VDH, respectively. Lane – and +, total protein obtained
742 from cells grown in the absence and presence of 5% methanol, respectively. (Right)
743 Expression profiles of PIP or VDH in *R. erythropolis* JCM3201 containing the
744 pCpi-QC1-PIP or pCpi-QC2-VDH, respectively. Total proteins (15 μg) were analyzed
745 by SDS-PAGE. Black and gray arrowheads indicate PIP and VDH, respectively. NC,
746 negative control. (C) Activity of PIP in *R. erythropolis* JCM3201 containing the
747 pIcl-QC1-PIP, pHN380 (20), or pCpi-QC1-PIP. The transformant was incubated in the
748 presence of 5% methanol for 24 h or 0.5 μg/μL thiostrepton for 20 h, and subjected to
749 PIP activity assay. NC, negative control, in which the total protein from *R. erythropolis*
750 JCM3201 containing an empty vector was used.

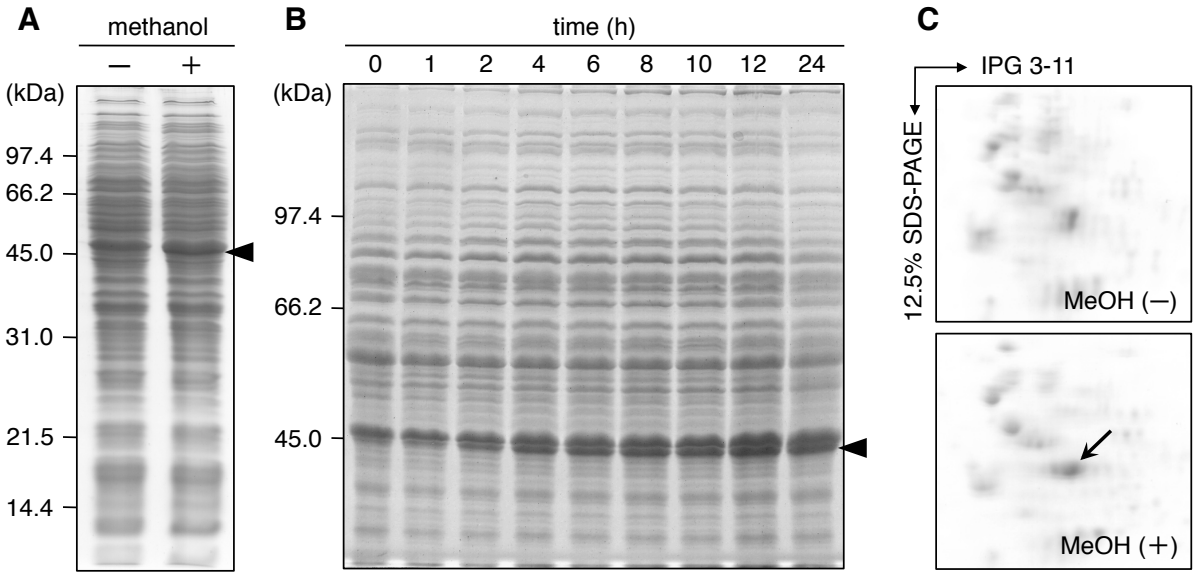
A
methanol
—
+
(kDa)
97.4
66.2
45.0
31.0
21.5
14.4
B
time (h)
0
1
2
4
6
8
10
12
24
(kDa)
97.4
66.2
45.0
C
IPG 3-11
12.5% SDS-PAGE
MeOH (—)
MeOH (+)

Fig. 1

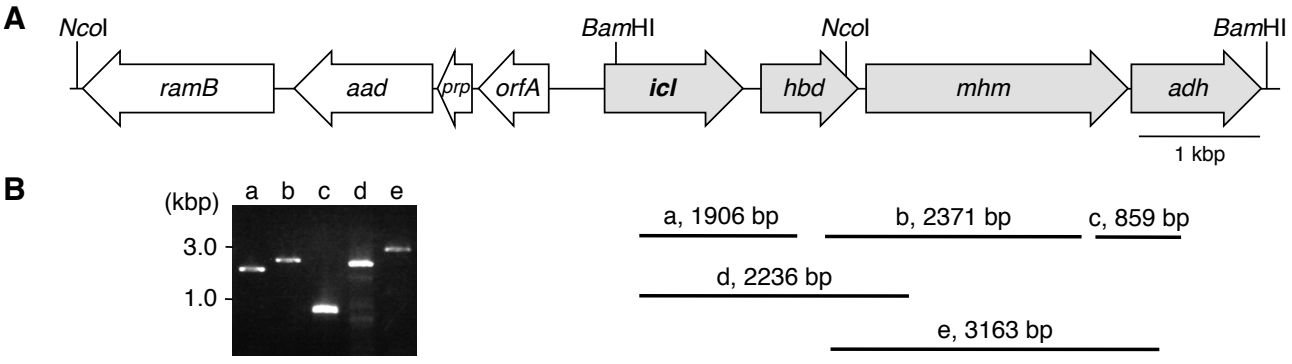
A
NcoI
BamHI
NcoI
BamHI
ramB
aad
prp
orfA
icl
hbd
mhm
adh
1 kbp
B
(kbp)
a
b
c
d
e
3.0
1.0
a, 1906 bp
b, 2371 bp
c, 859 bp
d, 2236 bp
e, 3163 bp

Fig. 2

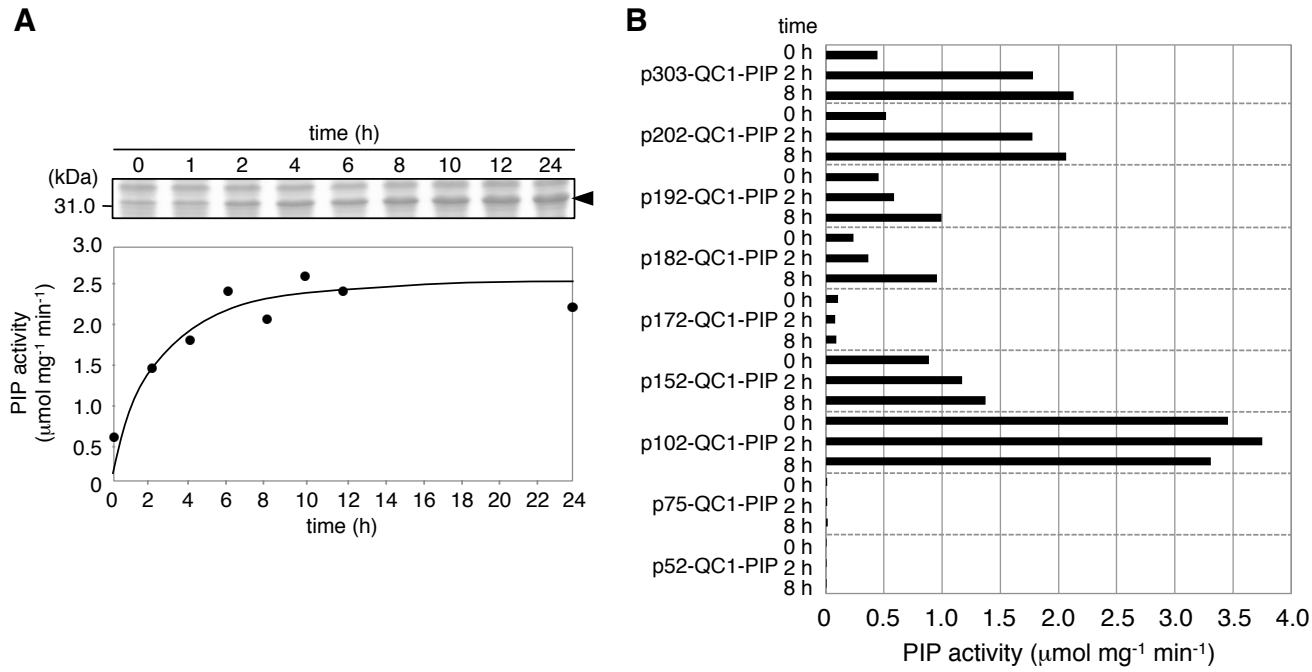
A
time (h)
0 1 2 4 6 8 10 12 24
(kDa)
31.0
PIP activity (μmol mg-1 min-1)
time (h)
B
time
0 h
p303-QC1-PIP 2 h
8 h
p202-QC1-PIP
p192-QC1-PIP
p182-QC1-PIP
p172-QC1-PIP
p152-QC1-PIP
p102-QC1-PIP
p75-QC1-PIP
p52-QC1-PIP
PIP activity (μmol mg-1 min-1)

Fig. 3

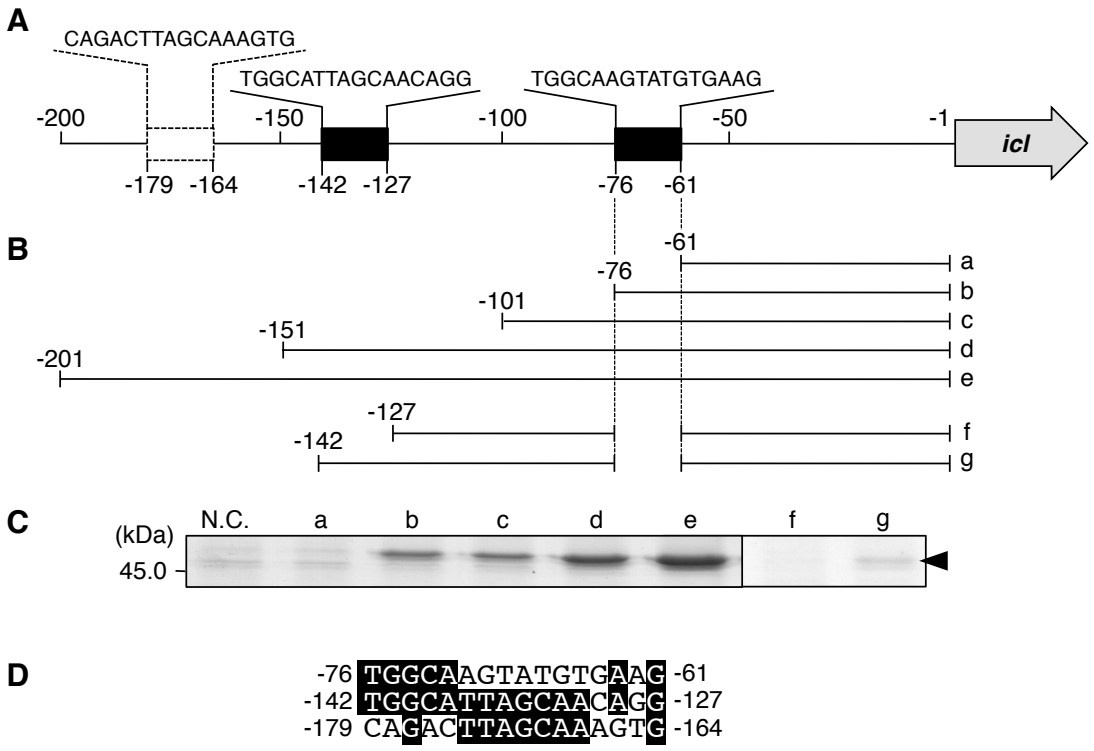
A
CAGACTTAGCAAAGTG
TGGCATTAGCAACAGG
TGGCAAGTATGTGAAG
-200
-150
-100
-50
-1
icl
-179 -164
-142 -127
-76 -61
B
-61
-76
-101
-151
-201
-127
-142
a
b
c
d
e
f
g
C
N.C.
(kDa)
45.0
D
-76 TGGCAAGTATGTGAAG -61
-142 TGGCATTAGCAACAGG -127
-179 CAGACTTAGCAAAGTG -164

Fig. 4

Fig. 5

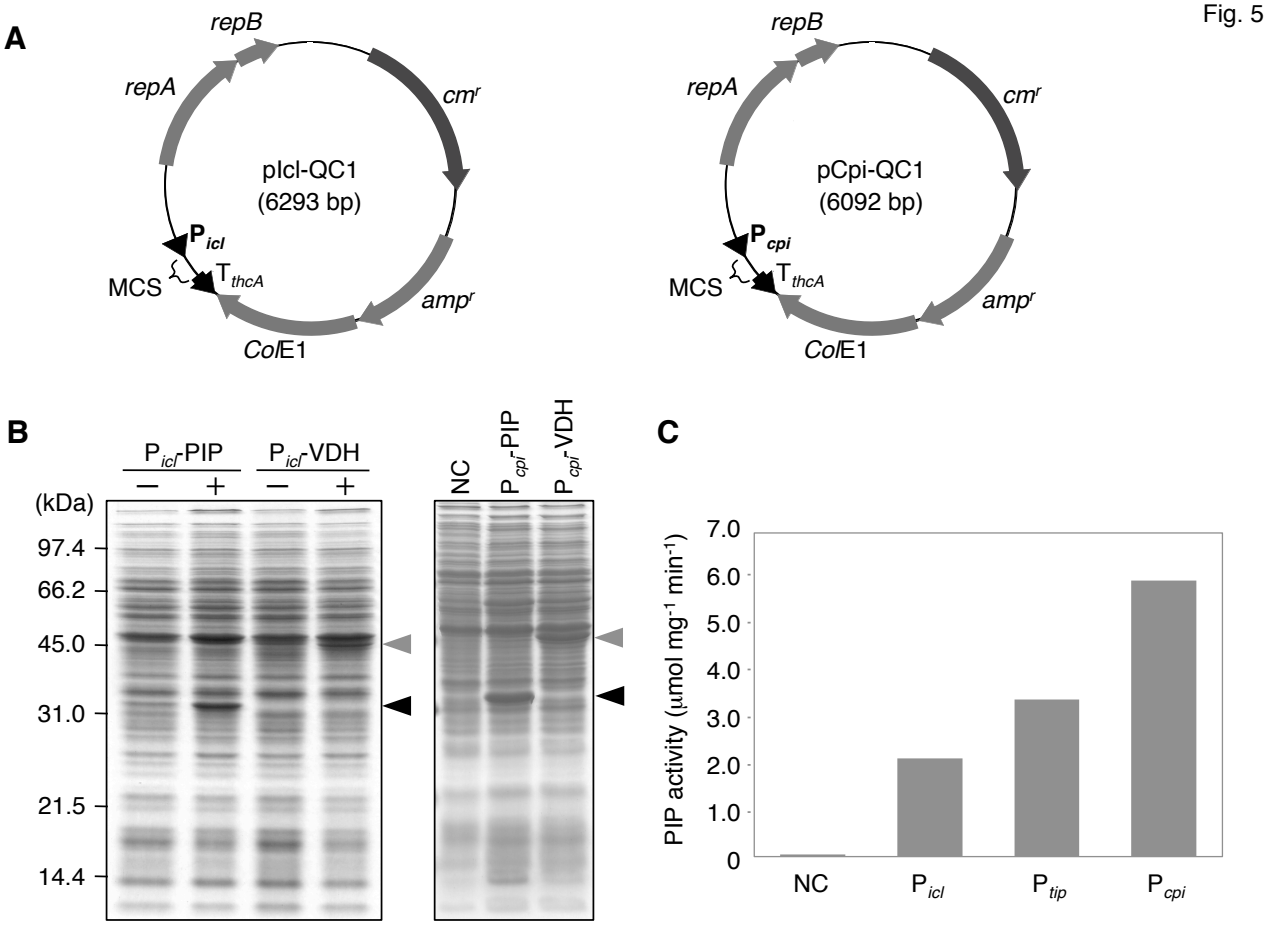
A
repB
repA
cmr
pIcl-QC1
(6293 bp)
Picl
MCS
TthcA
ampr
ColE1
repB
repA
cmr
pCpi-QC1
(6092 bp)
Pcpi
MCS
TthcA
ampr
ColE1
B
Picl-PIP
Picl-VDH
−
+
−
+
(kDa)
97.4
66.2
45.0
31.0
21.5
14.4
NC
Pcpi-PIP
Pcpi-VDH
C
PIP activity (μmol mg-1 min-1)
7.0
6.0
5.0
4.0
3.0
2.0
1.0
0
NC
Picl
Ptip
Pcpi

Table 1. Isocitrate lyase activities in total proteins of *R. erythropolis* PR4 wild-type and *ramB*$_{Re}$ knockout mutant grown with supplements and glucose

Growth supplements	*R. erythropolis* PR4	
	WT	*ramB*$_{Re}$KO
No supplement	8.4 ± 0.7	24.5 ± 2.6
1% Methanol	21.4 ± 3.8	21.4 ± 4.6
1% Sodium acetate	22.4 ± 2.0	23.4 ± 1.7
1% Glycerol	6.5 ± 0.5	ND
1% Glucose	5.4 ± 0.8	26.0 ± 3.1
1% Methanol and 1% glucose	6.4 ± 0.8	24.8 ± 5.6
1% Sodium acetate and 1% glucose	14.2 ± 2.4	23.6 ± 2.0
1% Glycerol and 1% glucose	5.7 ± 0.8	ND

Activities are indicated in U/mg protein: mean ± standard deviation. ND, not determined (n = 3).

Fig. S1. Expression vector construction and sequence of P_{icl}, P_{cpi}, MCS type1 and type2, and T_{thcA}. (A) Schematic map of expression vectors. Sixteen expression vectors were constructed, pIcl-QC1, pIcl-QC2, pIcl-QT1, pIcl-QT2, pIcl-RC1, pIcl-RC2, pIcl-RT1, pIcl-RT2, pCpi-QC1, pCpi-QC2, pCpi-QT1, pCpi-QT2, pCpi-RC1, pCpi-RC2, pCpi-RT1, and pCpi-RT2, which indicates Q, *repA* and *B*; R, *rep*; C, chloramphenicol-resistant; T, tetracycline-resistant; 1, MCS type1; 2, MCS type2, respectively. cm^r, chloramphenicol-resistant gene; tet^r, tetracycline-resistant gene (each pIcl and pCpi vector has either cm^r or tet^r); amp^r, ampicillin-resistant gene; *Col*E1, replication origin for *E. coli*; T_{thcA}, *thcA* transcriptional terminator; MCS, multiple-cloning site (each pIcl and pCpi vector has either MCS type1 or MCS type2); P_{icl}, 303-bp upstream region of icl_{Re}; P_{cpi}, 102-bp upstream region of icl_{Re}; *repAB* and *rep*, essential region for stable maintenance of the plasmid in *R. erythropolis*. (B) Sequences of P_{icl}, P_{cpi}, MCS, and T_{thcA}. All of the restriction enzyme sites indicated in the MCS, except for *Sna*BI in the R type vectors are unique. Gray arrows indicate the positions of the perfect IR sequences in the *thcA* terminator. Note that neither conserved Shine-Dalgarno sequence nor -35 and -10 promoter elements were found in the P_{icl} and P_{cpi}.

Fig. S2. Schematic drawing of the primary structure of $RamB_{Re}$, and alignment of its HTH domains. Black and gray boxes indicate the HTH and transcriptional regulation domains, respectively. Identical residues are shaded black, and similar residues are shaded gray. Abbreviations: aa, amino acids; RE, *R. erythropolis* PR4; MT, *M. tuberculosis*; CG, *C. glutamicum*. The HTH domain region is underlined.

Fig. S3. Comparison of icl_{Re} organizations in *R. erythropolis* PR4 and other bacteria. The gene names are as follows: *ramB*, transcriptional regulator involved in acetate metabolism; *aad*, acetamidase; *prp*, putative regulatory protein; *icl*, isocitrate lyase; *hbd*, 3-hydroxyacyl-CoA dehydrogenase; *mhm*, 5-methyltetrahydropteroyltriglutamate-homocysteine *S*-methyltransferase; *adh*, alcohol dehydrogenase; *abc*, branched-chain amino acid ABC transporter substrate-binding protein; *egc*, endoglycosylceramidase; *ndt*, Na^+-dependent transporter; *aceB*, malate synthase; *thiX*, protein potentially involved into thiamin biosynthesis; *lcoP*, ectoine betaine transporter; *umaA*, mycolic acid synthase; *dbp*, DNA binding protein. The ORF of white arrows indicate hypothetical protein; the ORF of black arrows indicate *icl* and *icl* homolog; and the ORF of gray arrows indicate *ramB* and *ramB* homolog.

A

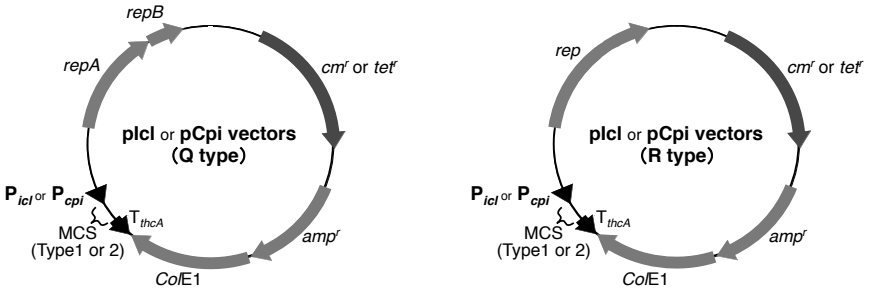

B

P_{icl}

BsrGI
TGT ACA GCG AAC TGC CGG AAT TTG CAA GTG GCG GAG TTG AGT GCA TTT CGT TCA CAG CCT GCG GTT TCT TTG CTA CTC GCC AGT ACG GAA CCT GTC CGA

TTG GGT AGT ACC AGC CGT GTA GGA ATC TTC ACA GAC TTA GCA AAG TGT GTT GAA AAG GTA GCG AAG ATT GGC ATT AGC AAC AGG TAG ACG GCA CTT TTT

CGA TGT GCC ATT CTC GGT AAG TAC ACA AGA AGG GCC TGG CAA GTA TGT GAA GTA GTA CGC ACG TAC TGC TCA CAA CAG GCC GGA CCA GCA GAT CAA AGA

GAT GGA GTC TTG

P_{cpi}

BsrGI
TGT ACA ATT CTC GGT AAG TAC ACA AGA AGG GCC TGG CAA GTA TGT GAA GTA GTA CGC ACG TAC TGC TCA CAA CAG GCC GGA CCA GCA GAT CAA AGA GAT

GGA GTC TTG

MCS Type 1

NcoI NdeI EcoRI SnaBI NotI BamHI HindIII BglII XhoI
GCC ATG GGC CAC CAT CAC CAT CAC CAT ATG GGA ATT CTA CGT AGC GGC CGC GGA TCC AAG CTT AGA TCT CTC GAG CAT CAC CAT CAC CAT CAC TGA
Met Gly His His His His His His Met Gly Ile Leu Arg Ser Gly Arg Gly Ser Lys Leu Arg Ser Leu Glu His His His His His His *

MCS Type 2

NdeI NcoI EcoRI SnaBI NotI BamHI HindIII BglII XhoI
CAT ATG GGC CAT CAC CAT CAC CAT CAC GCC ATG GGA ATT CTA CGT AGC GGC CGC GGA TCC AAG CTT AGA TCT CTC GAG CAT CAC CAT CAC CAT CAC TGA
Met Gly His His His His His His Ala Met Gly Ile Leu Arg Ser Gly Arg Gly Ser Lys Leu Arg Ser Leu Glu His His His His His His *

T_{thcA}

SpeI SalI
ACT AGT CGA CCC ACC GGC ACC CGT GAG CCC CTC GCT GCG GGT GCC GGT GCG AGG GAC TGC AAC ACG CGA AAC CTG CAC AAA CAC ACG GAG GTT GGA ATG

AGC GCC ACG GAC ACA CCC GAT ACC GGC GCC GTT CCA CCC CGG TTG GTG ACC ACC GCT GGG GCG GCT GAC CTG CTA CGC CGC CTC AGC GGG ACT CTA GT

Fig. S1

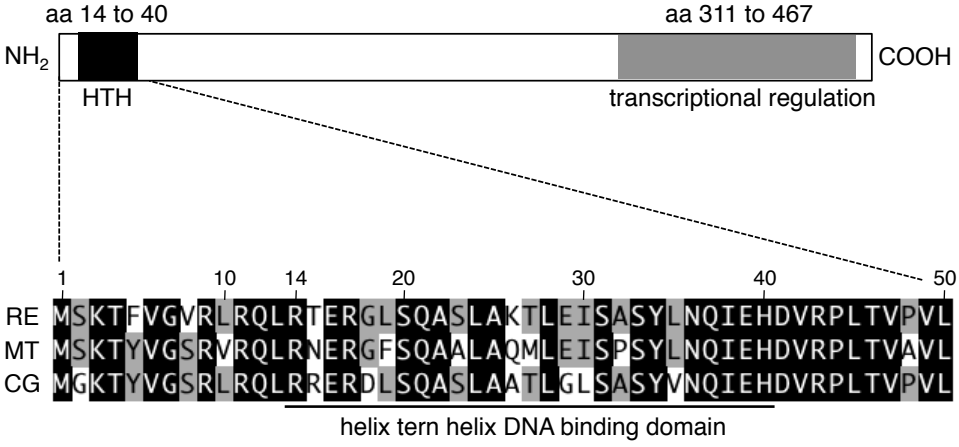

Fig. S2

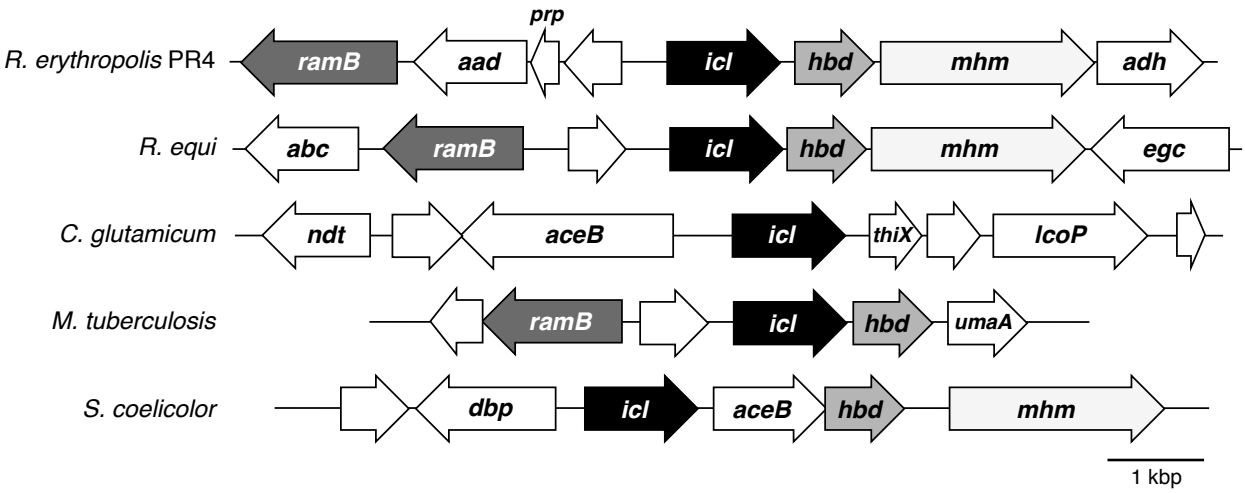
R. erythropolis PR4
ramB
aad
prp
icl
hbd
mhm
adh
R. equi
abc
ramB
icl
hbd
mhm
egc
C. glutamicum
ndt
aceB
icl
thiX
lcoP
M. tuberculosis
ramB
icl
hbd
umaA
S. coelicolor
dbp
icl
aceB
hbd
mhm
1 kbp

Fig. S3